

Bifurcation Spiking Neural Network

Shao-Qun Zhang, Zhi-Hua Zhou

National Key Laboratory for Novel Software Technology
Nanjing University, Nanjing 210023, China

{zhangsq,zhouzh}@nju.edu.cn

Abstract

Recently spiking neural networks (SNNs) have received much attention because of its rich biological significance and its power in processing spatial and temporal information. However, most existing SNNs are *static* due to the fixed eigenvalues of spiking generation functions, which means that neurons fire spikes in a fixed frequency when receiving constant input signals. Thereby, the static SNNs are limited in scalability. In this paper, we clarify the bifurcation relationship that dynamic eigenvalues have a great influence on the neuron excitation frequency. And then we propose the *Bifurcation Spiking Neural Network* (BSNN) for developing a *dynamic* SNN. Different from traditional *static* SNNs, BSNN takes a bifurcation system with time-varying eigenvalues as the basic building block, thus it has more powerful flexibility and is able to handle data with complex nonlinear structures. Experiments on wide-range tasks have been conducted, including a delayed-memory XOR task, four image recognition datasets, and 25 UCR archive. The results show that the performance of BSNN is superior to the existing static SNN models.

Key words: Spiking neural network, leaky-and-firing neuron, bifurcation

1. Introduction

Understanding how to dynamically generate spikes according to environmental change is a fundamental problem in SNNs. Previous studies along this aspect have focused more attention on how to train a *static* SNN by tackling the non-differentiability and discontinuity of spikes [GK02, VGT05, GKNP14, Güt16]. Several recent works attempt to improve the flexibility of SNNs by exploiting *threshold dynamics*. For instances, lots of researchers elucidate the local dynamical mechanisms through a balance of excitation and inhibition [HDHM06, BDM13] and some models with BPTT use a non-negative gate function to generate

an active zone where the synaptic current can be activated in a gradual manner [HS18]. Although the dynamic firing threshold can affect the spike generation frequency, it is independent of the neuron equation, which results in SNNs still being limited in the terms of neuronal plasticity. Therefore, in order to improve the plasticity of SNNs, we need to explore the neurons with elastic structures rather than those with fixed eigenvalues.

In this work, we are going to develop a dynamic SNN model with *time-dependent eigenvalues*, which has hardly been studied. Our starting point is a seminal illustration of [CCL19], which reveals a general discovery that various eigenvalues of the neuron equation in SNNs have a great influence on the neuron excitation frequency. To introduce this in detail, we give two simulation examples, as shown in Figure 1. Figure 1(a) shows the relationship between the eigenvalue γ of LIF neurons and the spike generation frequency, where the frequency curve is monotonically increasing as the eigenvalue γ grows from -1 to 1. Another example is to investigate the *bifurcation* relationship between the neuron excitation frequency and eigenvalues when receiving different input signals. In Figure 1(b), neurons with various eigenvalues work differently when processing weak signals; while inputting high-value signals, the family of excitation frequency curves can be obviously divided into two categories according to the sign of eigenvalues. In summary, the LIF neuron in SNN has a *bifurcation* structure with respect to the eigenvalues where the neuron excitation frequency will transit from one state to another as the eigenvalue γ crosses 0. Therefore, not only the magnitude but also the sign of the eigenvalue will affect the efficiency of neurons. Furthermore, using the neurons with dynamic eigenvalues will improve the flexibility of SNNs for processing complex signals.

We propose the *Bifurcation Spiking Neural Network* (BSNN) for achieving a novel paradigm of *dynamic* SNNs. By employing the plastic neurons with time-dependent bifurcation eigenvalues, BSNN is capable of capturing the adaptive learning behavior of the neurons to the environmental change. Furthermore, we implement a multi-layer BSNN by its equivalent model, *Hybrid Spike Response Model* (HSRM), which is able to cope with the discontinuity and non-differentiability of spikes with scalable gradient calculations. Experimental results on simulated and practical tasks show the superiority of BSNN to several state-of-the-art static SNNs.

The rest of this paper is organized as follows. We first review the previous studies about static SNNs in Section 2. Section 3 introduces the dynamic bifurcation neurons of BSNN. Section 4 implements a multi-layer BSNN by HSRM. The experiments are conducted on several simulated and practical datasets

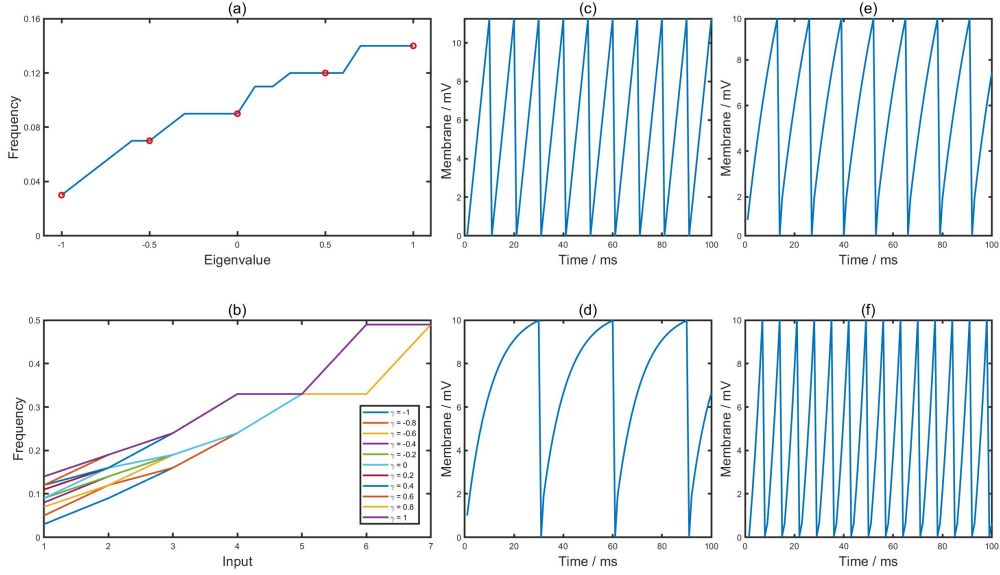


Figure 1: Simulation examples: (a) The schematic diagram of Eigenvalue-Frequency plot, (b) The Input-Frequency plot, (c)-(f) The time courses of the membrane potential with $\gamma = 0$, $\gamma = -1$, $\gamma = -0.5$, and $\gamma = 1$.

in Section 5. Finally, we conclude our work in Section 6.

2. Related Works

Recently the spiking neuron networks (SNNs) are frequently studied as models for networks of neurons in neuroscience. In contrast to most deep neural networks that use neurons with static nonlinearities that produce an analog output [Sch15], SNN is a dynamic system that transports information between neurons by firing time-dependent discontinuous spikes [GK02, VGT05, GKNP14, Güt16]. In general, the neuron models of SNNs are usually characterized as the first-order equations, such as the *leaky integrate-and-fire* (LIF) neurons.

Although SNN has a long history, there are great efforts on improving its performance. Early works along this aspect consider to add an absolute refractory period when the current membrane potential $u(t)$ hits the firing threshold u_{firing} [PMB12, HE15]. However, most studies are still about how to train SNN by ameliorating the conventional error backpropagation to overcome the non-differentiability of spikes.

Existing SNN training methods can be roughly divided into three categories. The first category aims at exploring a simple continuous-valued ANN and converting this deep ANN to accurate spiking equivalents

[ONL⁺13, EAM⁺15, RLH⁺17]. The second category configures an SNN on discontinuous spike activities, such as, SpikeProp and its variants transfer the information in the timing of a single spike [BKLP02, MLB06]. However, SpikeProps are limited to single-spike learning, which causes a large number of neurons to be in a shutdown state. Recently, [JZL18] accounts for the temporal contribution of the given presynaptic spike train to the firings of the post-synaptic neuron. The third category attempts to train SNNs in a temporal manner [HS18, LDP16, SO18]. [HS18] presents a temporal gradient descent method, BPJT, with a differentiable formulation of spiking dynamics. Considering the discontinuities at spike times as noise, [LDP16] treats the membrane potentials of spiking neurons as differentiable signals. [SO18] incorporates the temporal dependency between spikes that the backpropagated error at a given time step should be affected by earlier spike inputs.

3. Bifurcation Spiking Neural Networks

This section introduces the *Bifurcation Spiking Neural Network* (BSNN), which employs *dynamic bifurcation* neurons rather than *static* LIF neurons as the basic building blocks of networks. The *bifurcation* in our work indicates that the working efficiency of neurons changes significantly when the eigenvalues of the neuron equations that evolve over time pass through the critical point 0. We start from analyzing the working mechanism of *static* neurons, especially those with LIF neurons.

3.1. Eigenvalues and Neuron Excitation Frequency

Our starting point is a general discovery that the eigenvalues can affect the working efficiency of static neurons. In this subsection, we are going to clarify this finding by two simulated examples below. Before that, we need to review the LIF equation, which with input $I(t)$ and a rest voltage u_{rest} is generally formulated as follows:

$$\tau_m \frac{du}{dt} = u_{rest} + \gamma \cdot u + R \cdot I(t), \quad (1)$$

where $u(t)$ represents the membrane potential at time t , τ_m is the membrane time constant, γ is the self-decaying rate, usually preset to a negative constant, and R is the membrane resistance. Particularly, as a mathematical ODE model, the LIF equation has fixed negative eigenvalues γ by solving its algebraic formulation.

The first example is to investigate the relationship between eigenvalues γ of LIF equations and the neuron excitation frequency with constant input signals, which is shown in Figure 1(a). The frequency curve is monotonically increasing as the eigenvalue γ grows from -1 to 1. In detail, when $\gamma < 0$, the excitation frequency increases rapidly in the region far from 0, while is almost constant in the region near 0; relatively, when $\gamma > 0$, the excitation frequency changes sharply in the region close to 0, while becomes smoother in the region farther away from 0. We also plot the relationship between increasing input and the neuron excitation frequency with various eigenvalues. As shown in Figure 1(b), when receiving high-value signals, the family of excitation frequency curves will be obviously divided into two categories, that is, the frequency curves with positive eigenvalues will converge together and other curves with negative eigenvalues will be collected into another class. From a dynamic system perspective, the LIF neurons possess the *bifurcation* structures with respect to the eigenvalues;; with comparison of the critical case that $\gamma = 0$ in Figure 1(c), the neurons will be activated frequently in Figure 1(f) when the eigenvalues are greater than 0, while the eigenvalues are negative, the dynamic system enters the "inefficient" mode of operation, as shown in Figure 1(d) and 1(e).

Based on these above examples, we can confirm that the eigenvalues of neuron equations indeed have a great influence on the efficiency of neurons; both the magnitude and sign of the eigenvalue will affect the generation frequency of the spikes. By contrast, the static SNNs with fixed eigenvalues can only handle simple-mode signals. Thereby, developing plastic neurons with dynamic eigenvalues that can change according to time is significant for improving the adaptive learning flexibility of SNNs. However, it is not feasible to directly replace the original fixed constant γ in Equation 1 with a time-dependent function $\gamma(t)$, because the elastic self-decay rate will result in inaccurate calculation about the last firing time t^{firing} according to the closed-form solution shown in Equation 2.

$$u(t) = \exp(-\gamma(t) \frac{t - t^{firing}}{\tau_m}) \cdot [u_{rest} + \frac{R}{\tau_m} \int_0^{t-t^{firing}} \exp(\gamma(t) \frac{s}{\tau_m}) I(t-s) ds]. \quad (2)$$

3.2. Basic Bifurcation Neurons

We bridge this gap by exploiting some more complex dynamic neuron models, which not only maintain bifurcation eigenvalues but also have concise analytical solutions. Equation 3 illustrates such a dynamic bifurcation system with respect to the membrane potential $u(t)$ [Onu02, Kuz13].

$$\tau \frac{\partial u}{\partial t} = -\gamma u + \lambda u^* + g(t), \quad (3)$$

where γ is the self-decay rate ($\gamma > 0$), \mathbf{u}^* portrays the mutual promotion between neurons, which is usually expressed as the high-order term of $|\mathbf{u}|$, $\mathbf{g}(t)$ denotes the presynaptic input that consists of synaptic voltage and external signal, and $\boldsymbol{\lambda}$ is the control hyperparameters that change according to time. Assume that $u_i^* = \sum_{j \neq i} u_j + o(|u_i|)$ [MW05], where $o(\cdot)$ is the high-order term of u_i , then Equation 3 could be rewritten as

$$\begin{cases} \tau_1 \frac{\partial u_1}{\partial t} = -\gamma u_1 + \lambda_1 \left(\sum_{j \neq 1} u_j \right) + o(|u_1|) + g_1(t) \\ \vdots \\ \tau_n \frac{\partial u_n}{\partial t} = -\gamma u_n + \lambda_n \left(\sum_{j \neq n} u_j \right) + o(|u_n|) + g_n(t) \end{cases}.$$

By solving the algebraic formulation of Equation 3, we can obtain its analytical solution and the bifurcation structure.

Theorem 1 *If the control hyperparameter $\lambda_i \geq 0$, then there are at most 2^{n-1} bifurcation states in Equation 4, which is the algebraic formulation of Equation 3.*

$$\frac{d\mathbf{u}}{dt} = L_{\boldsymbol{\lambda}} \mathbf{u} + G(\mathbf{u}, \boldsymbol{\lambda}), \quad (4)$$

where

$$L_{\boldsymbol{\lambda}} = A + B_{\boldsymbol{\lambda}}, \quad G(\mathbf{u}, \boldsymbol{\lambda}) = o(|\mathbf{u}|)$$

and

$$A = \begin{pmatrix} -\gamma & & \\ & \ddots & \\ & & -\gamma \end{pmatrix}, \quad B_{\boldsymbol{\lambda}} = \begin{pmatrix} 0 & \lambda_1 & \cdots & \lambda_1 \\ \lambda_2 & 0 & \cdots & \lambda_2 \\ \vdots & \vdots & \ddots & \vdots \\ \lambda_n & \lambda_n & \cdots & 0 \end{pmatrix}.$$

On the basis of the results of Theorem 1, we can achieve dynamic eigenvalues with a series of time-dependent non-negative hyperparameters $\boldsymbol{\lambda}(t)$.

The logic flow of Theorem 1 can be roughly proved by the following two steps. First, finding the

characteristic roots of our proposed bifurcation neuron model. According to Equation 3, we can obtain its algebraic representation as follows:

$$\frac{d\mathbf{u}}{dt} = L_{\boldsymbol{\lambda}}\mathbf{u} + G(\mathbf{u}, \boldsymbol{\lambda}), \quad (5)$$

where

$$L_{\boldsymbol{\lambda}} = A + B_{\boldsymbol{\lambda}}, \quad G(\mathbf{u}, \boldsymbol{\lambda}) = o(|\mathbf{u}|)$$

and

$$A = \begin{pmatrix} -\gamma & & & \\ & \ddots & & \\ & & -\gamma & \end{pmatrix}, \quad B_{\boldsymbol{\lambda}} = \begin{pmatrix} 0 & \lambda_1 & \cdots & \lambda_1 \\ \lambda_2 & 0 & \cdots & \lambda_2 \\ \vdots & \vdots & \ddots & \vdots \\ \lambda_n & \lambda_n & \cdots & 0 \end{pmatrix}.$$

Suppose that the eigenvalues of the matrix $B_{\boldsymbol{\lambda}}$ are β_1, \dots, β_n . So we can have the following conclusion.

Lemma 1 *If the hyperparameter $\lambda_i \geq 0$, then the matrix $B_{\boldsymbol{\lambda}}$ has n real eigenvalues.*

Based on the results of Lemma 1, we can claim that the eigenvalue ρ_k^i of $L_{\boldsymbol{\lambda}}$ can be represented as the sum of that of A and that of $B_{\boldsymbol{\lambda}}$, that is,

$$\rho_k^i = -\alpha_k + \beta_i.$$

Next, we can elucidate the bifurcation states of the eigenvalues. For simplicity, we take the 2-neuron model as an example, in other words,

$$A = \begin{pmatrix} -\gamma & 0 \\ 0 & -\gamma \end{pmatrix}, \quad B_{\boldsymbol{\lambda}} = \begin{pmatrix} 0 & \lambda_1 \\ \lambda_2 & 0 \end{pmatrix}.$$

Let

$$\begin{cases} C_k = 2\gamma \\ D_k = \gamma^2 - \lambda_1\lambda_2 \end{cases},$$

then when $\Delta = C_k^2 - 4D_k = \lambda_1\lambda_2 \geq 0$, L_{λ} has two series of real eigenvalues:

$$\rho_k^1 = \frac{-C_k - \sqrt{C_k^2 - 4D_k}}{2},$$

and

$$\rho_k^2 = \frac{-C_k + \sqrt{C_k^2 - 4D_k}}{2}.$$

Obviously, ρ_k^1 must be less than zero, but it is not necessary for ρ_k^2 . Let $\lambda_c = \gamma^2$ be the bifurcation threshold, then for every $k \in \mathcal{N}$, the eigenvalues are on the bifurcation states:

$$\rho_k^1 = \frac{-C_k - \sqrt{C_k^2 - 4D_k}}{2} < 0,$$

$$\rho_k^2 = \frac{-C_k + \sqrt{C_k^2 - 4D_k}}{2} \begin{cases} < 0, & \lambda_1\lambda_2 < \lambda_c; \\ = 0, & \lambda_1\lambda_2 = \lambda_c; \\ > 0, & \lambda_1\lambda_2 > \lambda_c. \end{cases}$$

When $\lambda_1\lambda_2 < \lambda_c$, both neurons work in the self-decay mode, such as the simulated examples in Figure 1(d)-(e); while $\lambda_1\lambda_2 > \lambda_c$, a new bifurcation phenomenon occurs, one neuron still works in a memory self-decay mode, but the other neuron appears to promote memory. The new bifurcation states are affected by the interaction between the target neuron self-decay and the positive memory provided by other neurons in the same working cluster. So such a cluster of neurons will exhibit multiple working modes under the control of hyperparameters λ . Generally, for the case of n neurons, the solution of Equation 4 possesses at most 2^{n-1} bifurcation states. ■

4. Hybrid Spike Response Model

This section implements the multi-layer BSNN with an equivalent model, the *Hybrid Spike Response Model* (HSRM). Subsection 4.1 introduces the multi-layer feedforward architecture of BSNNs. And we train the networks with a scalable backpropagation mechanism in subsection 4.2.

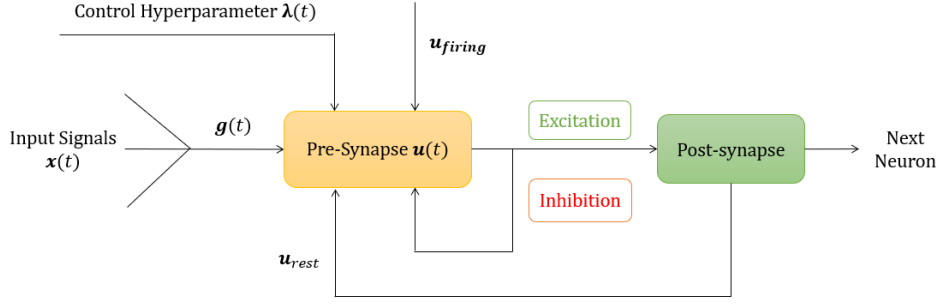


Figure 2: The workflow of neurons in a feedforward BSNN. Presynapse receives the input signals $\mathbf{x}(t)$ and integrates them as the pre-synaptic spikes $g(t)$. The middle neuron works in accordance with the bifurcation neuron equation, processing with all the information by switching the working modes. When the membrane potential $u(t)$ hits the firing threshold u_{firing} , the post-synaptic neuron is activated, then transmits the output signals to the next layer and resets the membrane potential in the middle neurons to the rest voltage u_{rest} . If $u(t)$ does not exceed u_{firing} , then the post-synaptic neuron is on the inhibitory state.

4.1. Multi-layer Feedforward Architecture

BSNN takes a working cluster of bifurcation neurons in Equation 3 as the basic building block. As shown in Figure 2, continuous input signals $\mathbf{x}(t)$ are fed to Presynapse and integrated as the pre-synaptic stimuli $g(t)$. The Presynapse processes with these stimuli by control hyperparameters $\lambda(t)$ that are affected by the current input signals. The output signals are eventually transmitted to the next neuron by Post-synapse if the membrane potential $u(t)$ reaches the firing threshold u_{firing} .

To formalize this feedforward procedure, we generate an *Hybrid Spike Response Model* (HSRM), which is equivalent to our proposed BSNN. First of all, it is necessary to introduce a differential operator δ_t that indicates the spikes within the interval before time t , that is, $\delta_t x_i = \sum_{firing} \epsilon(t - t_k^{firing})$, where t_k^{firing} is the firing time of the neuron i and $\epsilon(t)$ is the Dirac-delta function. So the input spike train of neuron i can be written as $g_i(t) = f_g(W_i \cdot \delta_t \mathbf{x}) \in (-1, 1)$. Consider the third term of Equation 3, λ is the current control factors, $\lambda_i(t) = f_\lambda(U_i \cdot \mathbf{x}) \in (0, 1)$. And the mutual promotion from the j -th neuron to the i -th neuron is caused by the last spike of the neuron j , noted as $u_j(\hat{t}_j)$, where $\hat{t}_j = \max\{t_j | t_j^{firing} \leq t\}$. Then, for the i -th neuron in the hidden layer, we have

$$\tau_i \frac{du_i(t)}{dt} = -\gamma u_i(t) + f_\lambda(U_i \cdot \mathbf{x}) \cdot \left(\sum_{j \neq i} u_j(\hat{t}_j) \right) + f_g(W_i \cdot \delta_t \mathbf{x}) \quad (6)$$

Akin to the Spike Response Model (SRM) [Ger95], Equation 6 with its initial condition $u_i(\hat{t}_i) = 0$ has an

equivalent solution:

$$u_i(t) = \int_0^\infty K(t - \hat{t}_i, t') \cdot Q_i(t - t_k^{firing} - t') dt'. \quad (7)$$

Considering the additive contribution of the refractory potential, the total membrane potential of a neuron i which has fired its last spike is the sum of the synaptic term (described in Equation 7) and the refractory term (denoted as *refr*) [BKLP02], that is, *Hybrid Spike Response Model* (HSRM):

$$u_i(t) = \int_0^\infty K(t - \hat{t}_i, t') \cdot Q_i(t - t_k^{firing} - t') dt' + refr(t - \hat{t}_i), \quad (8)$$

It is clear that the standard BSNN model is a special case of the HSRM, for specification, with

$$\begin{cases} K(t, s) = a(t - s) \cdot \frac{a(s)}{\tau} \cdot \exp(-\frac{s}{\tau}), \\ Q_i(t) = f_\lambda(U_i \cdot \mathbf{x}) \cdot (\sum_{j \neq i} u_j(\hat{t}_j)) + f_g(W_i \cdot \delta_t \mathbf{x}). \end{cases} \quad (9)$$

The output spike is emitted whenever $u_i(t)$ reaches the firing threshold u_{firing} . More formally, we can define a *firing function* to smooth this procedure, $\hat{u} = firing(u)$. Different from traditional *integrate-and-fire* approaches, the derivative of $firing(u)$ is available [HS18]. Finally, a multi-layer feedforward BSNN is established.

4.2. Backpropagation in HSRM

BSNN with supervised signals can be optimized via error backpropagation. Summing up the loss of each target supervised signals $\mathbf{u}^{target}(t)$ results in the cost function of the HSRM model.

$$E(t) = \frac{1}{2} \sum_{i=1}^{n_l} (\hat{u}_i(t) - u^{target}(t))^2, \quad (10)$$

where n_l is the number of neurons in l -th hidden layer. So for the i -th neuron, we have

$$\frac{\partial E(t)}{\partial W_{ik}} = \frac{\partial E(t)}{\partial \hat{u}_i} \cdot \frac{\partial \hat{u}_i}{\partial u_i} \cdot \frac{\partial u_i}{\partial W_{ik}} \quad (11)$$

As shown in Figure 2, the first term of Equation 11 represents the error backpropagation of the excitatory neurons, while the third term is the backpropagation of basic bifurcation neuron error. Plugging Equation 7

and Equation 10 into Equation 11, the gradient term can be calculated as:

$$\frac{\partial E}{\partial W_{ik}} = (\hat{u}_i - u^{target}) \cdot gate'(u_i) \cdot K_i * f'_g \cdot \delta_t x_k. \quad (12)$$

Similar to the error-backpropagation process with respect to W , the correction formula with respect to U_{ik} is given by:

$$\frac{\partial E}{\partial U_{ik}} = (\hat{u}_i - u^{target}) \cdot gate'(u_i) \cdot K_i * f'_{\lambda_i} \cdot \sum_{j \neq i} u_j(\hat{t}_j) \cdot x_k. \quad (13)$$

In general, we can also add a learning rate η on Equation 12 and 13 to help convergence, just like most deep artificial neural networks.

5. Experiments

In this section, we conducted experiments on several tasks to evaluate the functional performance of BSNN.

5.1. Delayed-memory XOR Task

We first consider a *Delayed-memory XOR* task, which performs the XOR operation on the input history stored over an extended duration [HS18, ADM16]. Specifically, the network receives two binary pulse signals, + or -, through an input channel and a go-cue channel. When the network receives two input pulses between two go-cue pulses, it should output the XOR signal of both inputs. In other words, the network outputs a positive signal if the input pulses are of equal signs (+ + or - -), and a negative signal if the input pulses are of opposite signs (+ - or - +). If there is only one input pulse between two go-cue pluses, the network should generate a null output.

Based on the above introduction, we simulated a Delayer-memory XOR dataset, which consists of 2400 input signals with 300 pulses, 2400 go-cue signals with 200 pulses, and the corresponding output signals. We also train the networks with the rest voltage $u_{rest} = 0$ by the first 2160 units and predict the output signals of the last 240 signals.

Figure 3 shows the experimental results of the BSNN model and the traditional SNN models on delayed-memory XOR task, in which BSNN can be highly qualified with the correct outputs, whereas the static-LIF

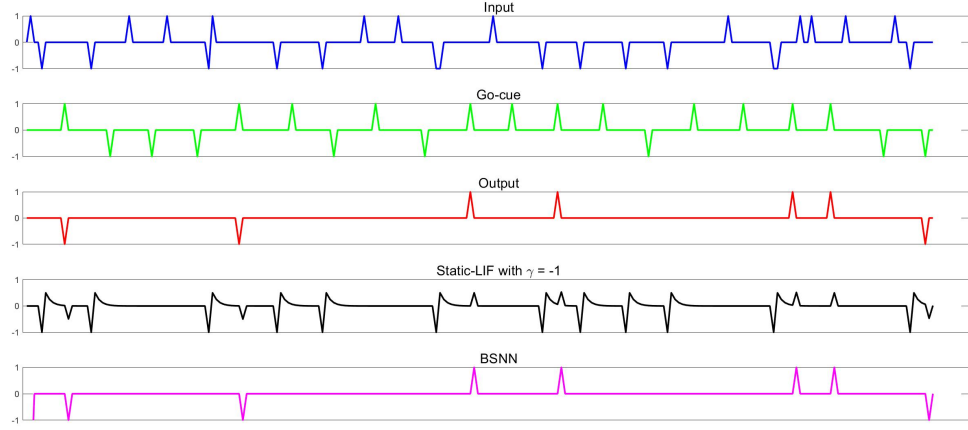


Figure 3: *Delayed-memory XOR task. The panels from top to bottom are the single-trial input, go-cue signals, output traces, the predictive signals of the static SNN, and the predictive signals of BSNN. BSNN is able to generate the correct signals, which only allows 1 to 2 units of delay. In contrast, the static-LIF SNN model with $\gamma = -1$ frequently makes mistakes because it cannot distinguish the effects of the input signals and the go-cue signals.*

spiking neural networks, even using BPTT with dynamic firing threshold [HS18], cannot even distinguish the role of different channel signals. These comparative results confirm that our proposed BSNN can perform nonlinear computations over the extended time.

5.2. Benchmark Tasks

We also test the performance of BSNN on four benchmark datasets: the MNIST handwritten digit dataset [LBB⁺98] and the N-MNIST digit dataset [OJCT15], the Extended MNIST-Balanced (EMNIST-Bal) dataset, and the Extended MNIST-Digit (EMNIST-Dig) dataset [CATvS17]. The detailed introduction about these datasets can be found in Supplementary Material. Similar to the preprocessing process of other SNNs [JZL18, LDP16, SO18], the static digit images are converted into spike trains using Poission Sampling and a Dynamic Vision Sensor (DVS). Here we employ a three-hidden layer BSNN, where the first two hidden layers each have 500 neurons and the number of neurons in the last layer is equal to the number of output classes. The output label is the one with the greatest spike count.

The experimental results are listed in Table 1. BSNN achieves a very superior testing performance to the existing SNN approaches on these image recognition datasets. Although the classification accuracy is still not comparable to conventional ANNs, it is a laudable result for most SNNs.

Table 1: *The classification results on four benchmark datasets.*

Dataset	Model	Setting	Accuracy
MNIST	CNN-SVM[NS12]		0.9879
	Basic-LIF [EAM ⁺ 15]	500-500	0.9572
	Hybrid MLP [JZL18]	500-500	0.9886
	SNN [LDP16]	500-500	0.9864
	SLAYER [SO18]	500-500	0.9911
	BSNN (this work)	500-500	0.9922 \pm 0.0004
N-MNIST	CNN[NL16]		0.9874
	Basic-LIF [EAM ⁺ 15]	500-500	0.9172
	Hybrid MLP [JZL18]	500-500	0.9886
	SNN [LDP16]	500-500	0.9872
	SLAYER [SO18]	500-500	0.9918
	BSNN (this work)	500-500	0.9934 \pm 0.0012
EMNIST-Bal	EDEN [DB17]		0.8766
	Basic-LIF [EAM ⁺ 15]	500-500	0.7835
	BSNN (this work)	500-500	0.8052 \pm 0.0031
EMNIST-Dig	EDEN [DB17]		0.9921
	Basic-LIF [EAM ⁺ 15]	500-500	0.8241
	BSNN (this work)	500-500	0.8527 \pm 0.0109

5.3. UCR Tasks

To evaluate the effectiveness of our proposed BSNN model, we also run the experiments on the UCR archive ¹, which includes 128 time series classification and clustering tasks [CKH⁺15]. Each of the UCR tasks comes in two parts, a TRAIN partition and a TEST partition, which will be in the same format, but are generally of different sizes. For example, the `Adiac` dataset has two files, `Adiac_TEST.txt` and `Adiac_TRAIN.txt`. The UCR dataset is more complex and harder than MNIST image recognition because there is a temporal dimension of timestamp.

We first train a two-layer BSNN with the TRAIN files, and then calculate the classification accuracy of the BSNN on the corresponding TEST files. The number of neurons in the hidden layer is fixed at 200 and other parameters are set as follows: the firing threshold $u_{firing} = 1$, the rest voltage $u_{rest} = 0$, the learning rate $\eta = 0.1$, the self-decay rate $\gamma = 0.5$, and the iteration times is 100. In the test procedure, the test samples are fed to the BSNN one by one, and the output classes are determined by the Output-Layer neuron ID with the largest values of spikes. In addition, we also compare BSNN against other methods,

¹https://www.cs.ucr.edu/~eamonn/time_series_data_2018/

Table 2: The test accuracy for 25 UCR time series classification tasks.

Task	COTE	BOSS	DTW	DTW_C	TSBF	TSF	LS	FS	MCNN	SpikeProp	BPTT	BSNN
Adiac	0.767	0.780	0.694	0.611	0.751	0.738	0.561	0.486	0.769	0.571	0.611	0.609
Beef	0.867	0.800	0.664	0.667	0.713	0.701	0.762	0.563	0.663	0.612	0.712	0.679
CBF	0.999	1	0.997	0.994	0.999	0.961	0.994	0.947	0.998	0.852	0.822	0.910
ChlorineConcentration	0.710	0.660	0.648	0.650	0.664	0.742	0.651	0.572	0.833	0.963	0.977	0.987
CinCECGTorso	0.931	0.875	0.650	0.93	0.833	0.931	0.833	0.826	0.942	0.596	0.701	0.601
DiatomSizeReduction	0.918	0.953	0.967	0.933	0.874	0.891	0.967	0.883	0.976	0.803	0.818	0.868
ECGFiveDays	1	1	0.768	0.797	0.817	0.993	1	0.996	1	0.928	0.943	0.962
FaceAll	0.895	0.790	0.808	0.808	0.766	0.769	0.783	0.808	0.765	0.652	0.662	0.669
FaceFour	0.909	1	0.830	0.886	0.949	0.966	0.952	0.910	1	0.663	0.711	0.686
FiftyWords	0.808	0.700	0.69	0.765	0.806	0.723	0.768	0.510	0.806	0.806	0.766	0.808
Fish	0.954	0.949	0.823	0.846	0.920	0.846	0.934	0.803	0.949	0.966	0.934	0.949
Gunpoint	0.993	1	0.907	0.913	0.989	0.953	1	0.939	1	0.973	0.987	0.987
Haptics	0.512	0.464	0.377	0.412	0.400	0.435	0.468	0.484	0.470	0.533	0.512	0.575
InlineSkate	0.450	0.489	0.384	0.387	0.397	0.325	0.427	0.266	0.312	0.402	0.470	0.3577
Mallat	0.964	0.942	0.934	0.914	0.963	0.928	0.954	0.976	0.943	0.977	0.964	0.988
MedicalImages	0.742	0.712	0.737	0.747	0.731	0.768	0.730	0.567	0.740	0.462	0.514	0.484
MoteStrain	0.915	0.927	0.835	0.862	0.865	0.882	0.913	0.783	0.921	0.822	0.833	0.866
NonInvasiveFetalECGThorax1	0.909	0.839	0.790	0.811	0.862	0.896	0.766	0.811	0.936	0.902	0.912	0.883
NonInvasiveFetalECGThorax2	0.927	0.900	0.865	0.880	0.870	0.906	0.911	0.880	0.940	0.881	0.865	0.836
OliveOil	0.900	0.900	0.833	0.867	0.910	0.900	0.500	0.787	0.867	0.857	0.833	0.822
Symbols	0.954	0.968	0.950	0.948	0.966	0.878	0.964	0.932	0.951	0.688	0.646	0.679
Trace	0.990	1	1	0.960	0.980	1	1	0.998	1	1	0.998	1
TwoLeadECG	0.985	0.996	1	0.998	0.971	0.888	0.997	0.887	0.999	0.995	1	0.981
WordSynonyms	0.734	0.655	0.649	0.740	0.700	0.619	0.660	0.437	0.724	0.626	0.664	0.678
Yoga	0.887	0.919	0.834	0.844	0.841	0.851	0.850	0.751	0.888	0.922	0.961	0.955

including classical time series classification approaches, such as COTE, BOSS, DTW, DTW_c, TSBF, TSF, LS, and FS [FJ14, BLB⁺17], as well as the multi-scale convolutional neural networks (MCNN) [CCC16], SpikeProp [BKLP02] and BPTT [HS18].

Table 2 shows a comprehensive evaluation of all methods on 25 datasets of UCR archive. For each dataset, we bolded the best performing classifier (larger is better). We observe from Table 2 that: (1) BSNN is very competitive, achieving the highest accuracy on 5 datasets; (2) BSNN outperforms the basic-SRM SNN model and the basic-LIF SNN model on most datasets; (3) Compared with conventional deep artificial neural networks, there are still gaps for BSNN in specific real-world applications. So we can claim that our proposed BSNN can exact the underlying computational mechanism to some extent and outperform the traditional SNN models.

6. Conclusion and Discussions

In this article, we present the *Bifurcation Spiking Neural Network* (BSNN), a novel dynamic SNN model that can be applied to continous data with complex nonlinear structures and perform nonlinear computations over the extended time. BSNN takes bifurcation neurons with time-varying eigenvalues as the basic building

block and is able to automatically switch the working modes of each neuron according to real-time input signals. Moreover, we also generate the *Hybrid Spike Response Model* (HSRM) to implement a multi-layer BSNN. HSRM allows gradient calculation by using the familiar backpropagation rule, which can fully utilize the existing statistical optimization methods in deep learning framework. Finally, we demonstrate our model on a delayed-memory XOR task, four benchmark datasets and the UCR archive. The experimental results show the effectiveness of BSNN.

We provided a series of theoretical discussions about the bifurcation properties and capability of BSNN, including and not limited to the relationship between the characteristic roots of the neuron equations and the spike generation frequency, the working mechanism of the bifurcation neurons system, and how to calculate the gradient for training the BSNN. Besides, we also declare that our work doesn't aim at realizing a biological learning phenomenon but attempting to explore some new thoughts on spiking neural networks. In this situation, Equation 3 employs the time-varying mutual promotion between adjacent neurons only provides a paradigm of implementing dynamic bifurcation neurons. We are interested in scaling up our work.

References

- [ADM16] Larry F Abbott, Brian DePasquale, and Raoul-Martin Memmesheimer. Building functional networks of spiking model neurons. *Nature Neuroscience*, 19(3):350, 2016.
- [BDM13] David G Barrett, Sophie Denève, and Christian K Machens. Firing rate predictions in optimal balanced networks. In *Advances in Neural Information Processing Systems*, pages 1538–1546, 2013.
- [BKLP02] Sander M Bohte, Joost N Kok, and Han La Poutre. Error-backpropagation in temporally encoded networks of spiking neurons. *Neurocomputing*, 48(1-4):17–37, 2002.
- [BLB⁺17] Anthony Bagnall, Jason Lines, Aaron Bostrom, James Large, and Eamonn Keogh. The great time series classification bake off: A review and experimental evaluation of recent algorithmic advances. *Data Mining and Knowledge Discovery*, 31(3):606–660, 2017.
- [CATvS17] Gregory Cohen, Saeed Afshar, Jonathan Tapson, and André van Schaik. Emnist: An extension of MNIST to handwritten letters. *arXiv preprint arXiv:1702.05373*, 2017.
- [CCC16] Zhicheng Cui, Wenlin Chen, and Yixin Chen. Multi-scale convolutional neural networks for time series classification. *arXiv preprint arXiv:1603.06995*, 2016.
- [CCL19] Chi-Ning Chou, Kai-Min Chung, and Chi-Jen Lu. On the algorithmic power of spiking neural networks. In *10th Innovations in Theoretical Computer Science*, page 5, 2019.
- [CKH⁺15] Yanping Chen, Eamonn Keogh, Bing Hu, Nurjahan Begum, Anthony Bagnall, Abdullah Mueen, and Gustavo Batista. The UCR time series classification archive. 2015.
- [DB17] Emmanuel Dufourq and Bruce A Bassett. EDEN: Evolutionary deep networks for efficient machine learning. In *2017 Pattern Recognition Association of South Africa and Robotics and Mechatronics (PRASA-RobMech)*, pages 110–115, 2017.
- [EAM⁺15] Steve K Esser, Rathinakumar Appuswamy, Paul Merolla, John V Arthur, and Dharmendra S Modha. Backpropagation for energy-efficient neuromorphic computing. In *Advances in Neural Information Processing Systems*, pages 1117–1125, 2015.
- [FJ14] Ben D Fulcher and Nick S Jones. Highly comparative feature-based time-series classification. *IEEE Transactions on Knowledge and Data Engineering*, 26(12):3026–3037, 2014.

- [Ger95] Wulfram Gerstner. Time structure of the activity in neural network models. *Physical Review E*, 51(1):738, 1995.
- [GK02] Wulfram Gerstner and Werner M Kistler. *Spiking Neuron Models: Single Neurons, Populations, Plasticity*. Cambridge University Press, 2002.
- [GKNP14] Wulfram Gerstner, Werner M Kistler, Richard Naud, and Liam Paninski. *Neuronal dynamics: From single neurons to networks and models of cognition*. Cambridge University Press, 2014.
- [Güt16] Robert Güti. Neural computation: Spiking neurons can discover predictive features by aggregate-label learning. *Science*, 351(6277):1041, 2016.
- [HDHM06] Bilal Haider, Alvaro Duque, Andrea R Hasenstaub, and David A McCormick. Neocortical network activity in vivo is generated through a dynamic balance of excitation and inhibition. *Journal of Neuroscience*, 26(17):4535–4545, 2006.
- [HE15] Eric Hunsberger and Chris Eliasmith. Spiking deep networks with LIF neurons. *arXiv preprint arXiv:1510.08829*, 2015.
- [HS18] Dongsung Huh and Terrence J Sejnowski. Gradient descent for spiking neural networks. In *Advances in Neural Information Processing Systems*, pages 1440–1450, 2018.
- [JZL18] Yingyezhe Jin, Wenrui Zhang, and Peng Li. Hybrid macro/micro level backpropagation for training deep spiking neural networks. In *Advances in Neural Information Processing Systems*, pages 7005–7015, 2018.
- [Kuz13] Yuri A Kuznetsov. *Elements of applied bifurcation theory*, volume 112. Springer Science & Business Media, 2013.
- [LBB⁺98] Yann LeCun, Léon Bottou, Yoshua Bengio, Patrick Haffner, et al. Gradient-based learning applied to document recognition. *Proceedings of the IEEE*, 86(11):2278–2324, 1998.
- [LDP16] Jun Haeng Lee, Tobi Delbruck, and Michael Pfeiffer. Training deep spiking neural networks using backpropagation. *Frontiers in Neuroscience*, 10:508, 2016.
- [MLB06] Sam McKennoch, Dingding Liu, and Linda G Bushnell. Fast modifications of the spikeprop algorithm. In *The 2006 IEEE International Joint Conference on Neural Network Proceedings*, pages 3970–3977, 2006.

- [MW05] Tian Ma and Shouhong Wang. Dynamic bifurcation of nonlinear evolution equations. *Chinese Annals of Mathematics*, 26(02):185–206, 2005.
- [NL16] Daniel Neil and Shih-Chii Liu. Effective sensor fusion with event-based sensors and deep network architectures. In *2016 IEEE International Symposium on Circuits and Systems (ISCAS)*, pages 2282–2285, 2016.
- [NS12] Xiao-Xiao Niu and Ching Y Suen. A novel hybrid CNN-SVM classifier for recognizing handwritten digits. *Pattern Recognition*, 45(4):1318–1325, 2012.
- [OJCT15] Garrick Orchard, Ajinkya Jayawant, Gregory K Cohen, and Nitish Thakor. Converting static image datasets to spiking neuromorphic datasets using saccades. *Frontiers in neuroscience*, 9:437, 2015.
- [ONL⁺13] Peter O’Connor, Daniel Neil, Shih-Chii Liu, Tobi Delbruck, and Michael Pfeiffer. Real-time classification and sensor fusion with a spiking deep belief network. *Frontiers in Neuroscience*, 7:178, 2013.
- [Onu02] Akira Onuki. *Phase transition dynamics*. Cambridge University Press, 2002.
- [PMB12] H  lene Paugam-Moisy and Sander Bohte. Computing with spiking neuron networks. In *Handbook of Natural Computing*, pages 335–376. Springer, 2012.
- [RLH⁺17] Bodo Rueckauer, Iulia-Alexandra Lungu, Yuhuang Hu, Michael Pfeiffer, and Shih-Chii Liu. Conversion of continuous-valued deep networks to efficient event-driven networks for image classification. *Frontiers in Neuroscience*, 11:682, 2017.
- [Sch15] J  rgen Schmidhuber. Deep learning in neural networks: An overview. *Neural Networks*, 61:85–117, 2015.
- [SO18] Sumit Bam Shrestha and Garrick Orchard. Slayer: Spike layer error reassignment in time. In *Advances in Neural Information Processing Systems*, pages 1419–1428, 2018.
- [VGT05] Rufin VanRullen, Rudy Guyonneau, and Simon J Thorpe. Spike times make sense. *Trends in Neurosciences*, 28(1):1–4, 2005.